Differences in the Oligomeric States of the LDH-like L-MalDH from the Hyperthermophilic Archaea *Methanococcus jannaschii* and *Archaeoglobus fulgidus*

D. Madern,*,† C. Ebel,† H. A. Dale,‡ T. Lien,‡ I. H. Steen,‡ N.-K. Birkeland,‡ and G. Zaccai†

Laboratoire de Biophysique Moléculaire, Institut de Biologie Structurale, UMR 5075, CEA-CNRS-UJF, 41 rue Jules Horowitz, 38027 Grenoble Cedex 1, France, and Department of Microbiology, University of Bergen, Jahnebakken 5, P.O. Box 7800, N-5020 Bergen, Norway

Received January 25, 2001; Revised Manuscript Received April 24, 2001

ABSTRACT: L-Malate (MalDH) and L-lactate (LDH) dehydrogenases belong to the same family of NAD-dependent enzymes. To gain insight into molecular relationships within this family, we studied two hyperthermophilic (LDH-like) L-MalDH (proteins with LDH-like structure and MalDH enzymatic activity) from the archaea *Archaeoglobus fulgidus* (*Af*) and *Mehanococcus jannaschii* (*Mj*). The structural parameters of these enzymes determined by neutron scattering and analytical centrifugation showed that the *Af* (LDH-like) L-MalDH is a dimer whereas the *Mj* (LDH-like) L-MalDH is a tetramer. The effects of high temperature, cofactor binding, and high phosphate concentration were studied. They did not modify the oligomeric state of either enzyme. The enzymatic activity of the dimeric *Af* (LDH-like) L-MalDH is controlled by a pH-dependent transition at pH 7 without dissociation of the subunits. The data were analyzed in the light of the crystallographic structure of the LDH-like L-MalDH from *Haloarcula marismortui*. This showed that a specific loop at the dimer−dimer contact regions in these enzymes controls the tetramer formation.

The L-malate dehydrogenases catalyze the NAD(P)-dependent interconversion of oxaloacetate to malate. Analysis of various genome sequences have suggested that this activity is achieved by two nonhomologous groups of enzymes (*1*).

In the first group, proteins purified from *Methanothermus fervidus* (*Mf*),[1] *Methanobacterium thermoautotrophicum* (*Mt*), and *Methanococcus jannaschii* (*Mj*) present malate dehydrogenase activity (*2*−*4*). So far, however, precise information about the oligomeric state, phylogeny, and three-dimensional structure of these proteins is lacking. The attribution of the *Mj* protein (ORF 1425) as a MalDH remains controversial, since it was demonstrated that it can act on substrates other than malate or oxaloacetate (*4*).

Enzymes from the second group are incomparably better defined. They are members of a large NAD-dependent dehydrogenase family including L-lactate dehydrogenase (L-LDH) and alcohol dehydrogenase (ADH). A number of these L-MalDH have been purified, characterized, and sequenced from a wide variety of organisms (*5*). Solution studies have shown that they exist as dimeric or tetrameric strucures (*6*, *7*). Various crystallographic structures of bacterial and eucaryal dimeric L-MalDH have been described (refs *8* and *9* and references therein). Their phylogeny has shown that they cluster within the two large mitochondrial and cytosolic clades of L-MalDH (*10*). For the tetrameric L-MalDH, the crystallographic information is so far limited to a single Archaeal L-MalDH (*11*, *12*). The enzymatic mechanism of L-MalDH has been probed by using site-directed mutagenesis to modulate substrate specificity (*13*, *14*) and coenzyme preference (*15*). A structure that mimics the catalytic state has been trapped showing that a charge imbalance inside the catalytic vacuole is responsible for substrate discrimination (*16*). The activity of the monomeric state remains controversial (*17*−*19*). However, a dimeric species that condenses to form the tetrameric L-MalDH has been characterized to be active (*20*). Various biochemical studies and primary sequence determinations have suggested that a specific LDH-like group of enzymes within the L-MalDH might be considered (*13*, *21*−*25*).

To refine our understanding of the LDH-like L-MalDH we tried to establish if a strict oligomeric state/primary sequence correlation exists within this group. To achieve this, we used the recombinant hyperthermophilic LDH-like L-MalDH of *Methanococcus jannaschii* (*Mj*, ORF 0490) (*25*) and *Archaeoglobus fulgidus* (*Af*) (*24*). The oligomeric states of the *Af* and *Mj* (LDH-like) L-MalDH were determined in solution, at ambient temperature and 70 °C, with the aim to record if these enzymes displayed a thermal-dependent oligomeric state change as it was reported for various hyperthermophilic enzymes (*26*, *27*). This was done in analytical centrifugation (AUC) and small-angle neutron scattering (SANS) experiments, in order to overcome possible temperature or salt artifacts associated with the oligomeric state determination by size exclusion chromatography.

* Corresponding author. Fax: (33).(0).4.38.78.54.94. Tel: (33).(0).4.38.78.95.71. E-mail: madern@ibs.fr.

† Institut de Biologie Structurale.

‡ University of Bergen.

[1] Abbreviations: L-MalDH, L-malate dehydrogenase (EC 1.1.1.37); L-LDH, L-lactate dehydrogenase (EC 1.1.1.27); AUC, analytical ultracentrifugation; CD, circular dichroism; SANS, small-angle neutron scattering; *Hm*, *Haloarcula marismortui*; *Af*, *Archaeoglobus fulgidus*; *Mj*, *Methanococcus jannaschii*; *Mf*, *Methanothermus fervidus*; *Tm*, *Thermotoga maritima*; ADH, alcohol dehydrogenase.

10.1021/bi010168c CCC: $20.00
Published on Web 08/01/2001

Our results demonstrated that the *Mj* is a tetramer and that the *Af* enzyme is the first LDH-like L-MalDH characterized as a dimer. The results were analyzed with respect to biochemical and crystallographic properties of the well described tetrameric LDH-like L-MalDH from *Haloarcula marismortui* (*12*, *20*).

MATERIALS AND METHODS

Protein Preparation. The purification of recombinant *Mj* (LDH-like) L-MalDH has been described previously (*25*). The pT7-7 plasmid carrying the *Mj* enzyme was transformed into the BL21DE3 pLysS *Escherichia coli* (*E. coli*) cells prior to expression. The amplification, cloning, and expression of *Af* (LDH-like) L-MalDH gene were carried out as described in the instruction manual for the Invitrogen pBAD TOPO TA Cloning Kit, version C. The following primers were used: 5′ *TGA* ACA *AGG AGA TA*T ACA TATG AAA CTC GGT TTT GTT GGT GCG 3′ (italicized: a stop codon and a ribosome binding site); 5′ CT TGG ATC *CTA* ATA TCC GAG TTC CTC AAG CC 3′ (italicized: a stop codon). A PLATINUM *Taq* DNA polymerase High Fidelity (Gibco-BRL) was used for amplification. The pSJS1240 (*28*) was transformed into the One Shot *E. coli* cells prior to expression. The recombinant *Af* L-MalDH was purified to homogeneity by heat treatment, affinity chromatography (Red Sepharose CL-6B, Amersham Pharmacia Biotech), where the proteins were eluted with 10 mM L-malate and 1.0 mM NAD^+ in 50 mM sodium phosphate buffer pH 8.0, and anion exchange chromatography (HiTrap Q Sepharose, Amersham Pharmacia Biotech), where the proteins were eluted with a salt gradient of 1−20% of NaCl in 50 mM Tris/HCl buffer pH 8.1.

The recombinant *Af* L-MalDH displays the same features as the native *Af* L-MalDH with regard to thermostability and the effect of salts on thermostability.

Protein Concentration. The protein concentrations were calculated by assuming molar extinction coefficients determined from the primary sequence. They were 26150 and 8160 mol^{-1} L cm^{-1}, for *Af* and *Mj* (LDH-like) L-MalDH, respectively. The low value for the *Mj* enzyme is due to the lack of tryptophan residues in the sequence.

Enzymatic Assay. (a) Standard Assay. Enzyme solution was mixed with 1 mL of 0.1 M KCl and 50 mM Tris-HCl pH 8.0 supplemented with oxaloacetate (0.3 mM) and NADH (0.2 mM). The oxidation of NADH accompanying the conversion of oxaloacetate to malate was followed for both enzymes at 70 °C by measuring the decrease in absorbance at 340 nm using a Beckman DU 7500 spectrophotometer. The data were corrected for the thermal degradation of NADH.

(b) Effect of pH. The measurements were done in a mixture of 50 mM KH_2PO_4/K_2HPO_4 buffered at the chosen pH.

Sequence Alignment. An alignment of the three archaeal L-MalDH sequences was done using the clustal W method. It was modified by inspection according to the crystallographic information available for an LDH-like L-MalDH (*12*). Residue numbering is based on the system of L-LDH, which is also valid for the LDH-like group of L-MalDH (*12*).

Circular Dichroism Spectroscopy. A Jobin Yvon CD6 circular dichroism spectropolarimeter with thermostated sample holder was used. Data were recorded at 25 °C with an interval of 1 nm and an integration time of 2 s using cells of 0.1 cm optical pathlength. The protein concentration was 0.5 mg/mL in various solutions buffered at the chosen pH by a mixture of 50 mM KH_2PO_4/K_2HPO_4. Each spectrum is an average of three scans, corrected for buffer.

Small-Angle Neutron Scattering. Concentrated *Mj* and *Af* LDH-like L-MalDH samples were dialyzed at 4 °C, against 0.1 M KCl Tris-HCl pH 8, and diluted with the dialysate in 0.100 cm quartz cuvettes to obtain three protein concentrations in the 5−20 mg/mL range. Neutron scattering experiments were performed at the Institut Laue Langevin (Grenoble, France) on the instrument D11, using two sets of wavelength−collimation distance−sample−detector distance values, 10 Å−2.m−2.8 m and 7 Å−4.0 m−4.5 m, to cover a large scattering vector range. The detector was moved to 1.2 m to measure the background intensities scattered at larger angles, to verify that the scattering of the buffer was properly subtracted. The data were treated in a standard way, by subtracting the scattering of the buffer and dividing by that of 0.100 cm of water (H_2O) and calibrated by using the procedure described (*29*). The square of the apparent radius of gyration (Rg^2_{app}) and forward intensity $I(0)/c_2$ (c_2 is protein concentration) were obtained from Guinier plots (ln $I(Q)$ versus Q^2) in a $(Rg_{app})Q$ range of 0.3−1.3 ($Q = 4\pi(\sin\theta)/\lambda$, with θ equal to half the scattering angle) (*30*). The $I(0)/c_2$ and Rg^2_{app} values were extrapolated to zero protein concentration to correct for interparticle effects and to obtain the mean square radius of gyration (Rg^2) and forward scattered intensity corresponding to the particles in solution. The extrapolated forward scattered intensity is related to the molar mass, M_2, as follows:

$$(I(0)/c_2)_{c_2=0} = M_2(\partial\rho_N/\partial c_2)_\mu^{\,2}/N_A \qquad (1)$$

Here N_A is Avogadro's number and $(\partial\rho_N/\partial c_2)_\mu$ is the neutron scattering length density increment expressing the contrast between the particle and the solvent (*29*). When the solution contains different types of particle (e.g. tetramers and dimers), Rg^2_{app} and $(I(0)/c_2)_{c_2=0}$ correspond to weighted mean values that can be calculated from a model providing the relative concentrations of the different particles (30).

Sedimentation Velocity. Experiments were performed on a Beckman XLA analytical ultracentrifuge, equipped with a UV scanning system, using a four hole AN-60 Ti rotor with double centerpieces of 1.20 cm path length. In a typical experiment, 200 absorbance profiles for each sample were recorded at 42 000 rpm. The wavelengths were chosen according to the characteristics of the samples. The scan profiles were analyzed from 8 scans recorded in the range 83−122 min with *Mj* LDH-like L-MalDH and in the range 59−87 min with the *Af* enzyme using the time derivative software dcdt+ (*31*). The derivative profiles showed, unless otherwise mentioned, a symmetrical peak whose position was used to calculate the experimental sedimentation coefficient s_{exp}. We used the program Sednterp (developed by D. B. Haynes, T. Laue, and J. Philo; http://www.bbri.org/RASMB/rasmb.html) to calculate partial specific volumes $\bar{v}_2$, hydration B_1, and solvent densities ρ and viscosities η. The corrected coefficients, $s_{20\ w}$, were calculated using $\bar{v}_2 = 0.7502$ for *Mj* L-MalDH and 0.7479 for *Af* L-MalDH and hydration $B_1 = 0.41$ g of water/g of protein for both enzymes.

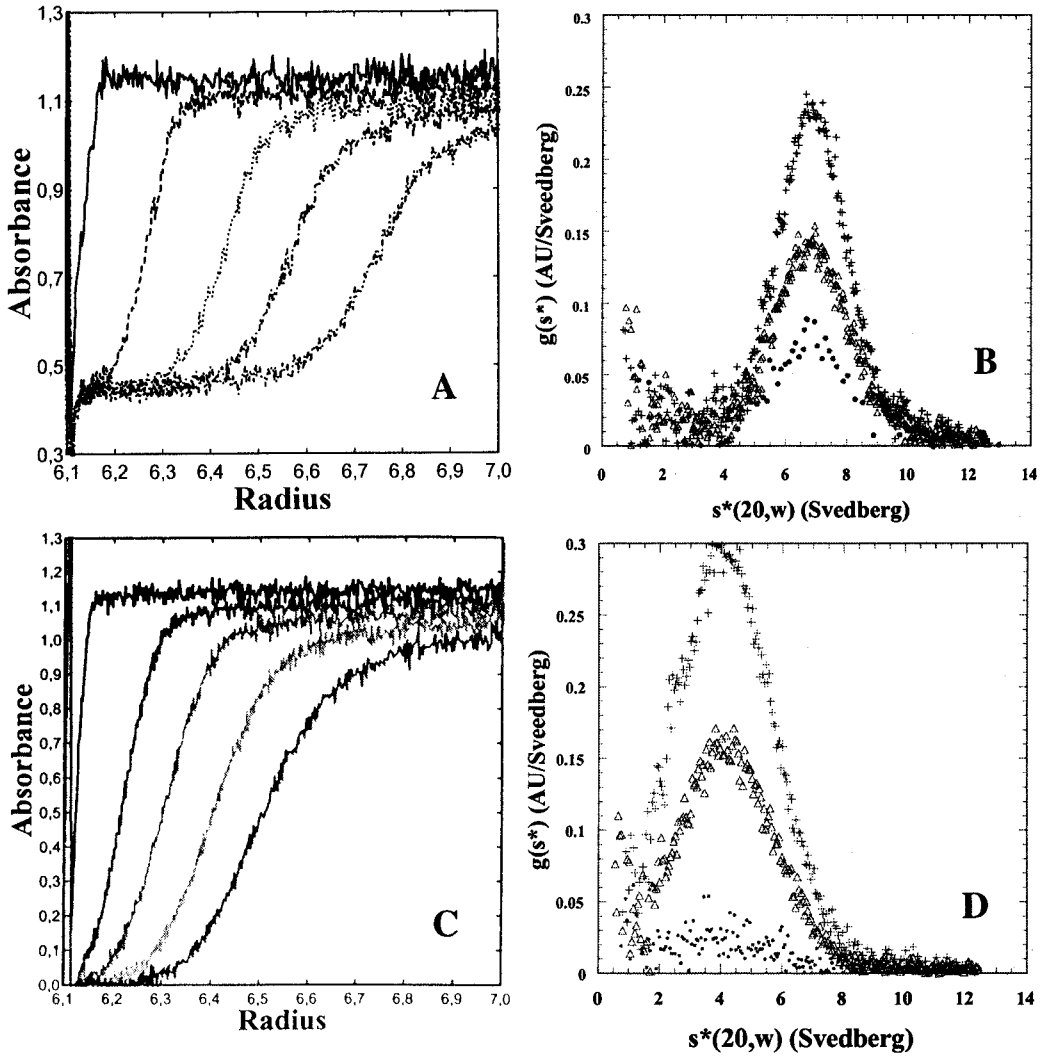

FIGURE 1: Sedimentation analysis of the *A. fulgidus* and *M. jannaschii* LDH-like L-MalDH. The sedimentation profile of scans recorded at time = 0, 30, 60, 90, and 120 min were monitored at 20 °C as described in Materials and Methods: panel A, *M. jannaschii*; panel C, *A. fulgidus*. The *Mj* $g(s^*)$ distribution at 5, 3, and 1 mg/mL (+, Δ, ●) is shown in panel B. The *Af* $g(s^*)$ distribution at 5, 1, and 0.1 mg/mL (+, Δ, ●) is shown in panel D.

In the case of the 0.88 M K_2HPO_4 solution, a density of 1.124 316 g/cm^3 and a viscosity of 1.424 mPa s were determined experimentally using an ANTON PAAR DMA 500 density meter and an ANTON PAAR AMV 200 automated microviscosimeter, respectively.

Corrected $s_{20\,w}$ were calculated using eq 2 since protein hydration has to be considered in solution as having a density significantly higher than water. This was the case with phosphate solution of 0.48 and 0.88 M. $\bar{v}_1 = 1$ mL/g is the partial specific volume of water.

$$s_{20\,w} = s_{exp}(\eta/\eta_{w,20})(1 - \rho_{w,20}\bar{v}_2)/[(1 + B_1) - \rho(\bar{v}_2 + B_1\bar{v}_1)] \quad (2)$$

RESULTS

Analytical ultracentrifugation (AUC), at 25 °C, and small-angle neutron scattering (SANS) at 70 °C experiments were used to investigate the structural properties of the *Mj* and *Af* (LDH-like) L-MalDH.

Mj LDH-like L-*MalDH Is a Tetramer*. The 200 boundary profiles were recorded during ultracentrifugation at three different concentrations of the *Mj* LDH-like L-MalDH. To ensure a direct comparaison of the respective *Mj* and *Af* sedimentation velocities, only five boundary profiles, recorded at constant intervals of time, are shown in Figure 1 (panel A, C).

The $g(s^*)$ profiles calculated for the *Mj* enzyme are shown in Figure 1 (panel B). The peaks are always centered at the same position, indicating that the *Mj* LDH-like L-MalDH does not dissociate when the protein concentration decreases. The data were well fitted with a main species corresponding to the *Mj* LDH-like L-MalDH and a small heterogeneity corresponding to less than 5% of the signal. The calculated $s_{20,w}$ values in 0.1 M KCl displayed a linear relationship in the protein concentration range from 0.05 up to 5 mg/mL (Figure 2). The value extrapolated to zero concentration ($s_{20,w} = 6.9$ S) is in agreement with the $s_{20,w} = 7$ measured for the tetrameric wild-type *Hm* LDH-like L-MalDH (*20*), consistent with a tetrameric structure for the *Mj* enzyme. A calculated molecular mass of 113 kDa was found, lower than but similar to the expected value of 137 kDa. The difference is probably due to a very small sample heterogenity.

The analytical centrifuge cannot reach a temperature above 40 °C. We chose, therefore, to monitor the *Mj* LDH-like

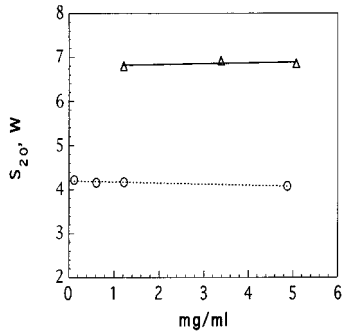

FIGURE 2: Effect of protein concentration on the sedimentation coefficient of *A. fulgidus* and *M. jannaschii* LDH-like L-MalDH. The $s_{20,w}$ values for *Af* (circles) and *Mj* (triangles) were derived at 20 °C, from the major peaks generated from the time derivative analysis.

L-MalDH oligomeric state at a higher temperature by using SANS. The experiments were performed at 70 °C; a higher temperature could not be reached due to the design of the sample holder on the neutron small-angle camera. Radii of gyration (Rg_{app}) and forward scattered neutron intensity values were recorded in a protein concentration range from 5 to 15 mg/mL. With the *Mj* LDH-like L-MalDH, the Rg_{app} values of 35 and 33 Å obtained at 25 and 70 °C, respectively, are in accordance with those expected for a tetrameric enzyme. The Rg_{app} value of 35 Å determined at 25 °C with the *Mj* LDH-like L-MalDH is larger than that of tetrameric *Hm* enzyme, 30 Å (*7*). The apparent Rg_{app} and forward scattered intensity, which increase at higher protein concentrations and at 70 °C, reflect the tendency of *Mj* LDH-like L-MalDH to aggregate. This phenomenon was confirmed by the precipitate observed in the measuring cell at 10 mg/mL after 2 h incubation at 70 °C. The forward scattered intensity ($I(0)/c_2$) value is directly related to the molar mass. The values found are about 20% lower than expected, suggesting a systematic 20% overestimation of the *Mj* extinction coefficient, by the sequence analysis method. The difficulty in the measurement of the sample concentration is related to the lack of W residues in the sequence.

Af LDH-like L-MalDH Is a Dimer under All Conditions Tested. The boundary profiles recorded for *Af* LDH-like L-MalDH at various constant intervals of time during ultracentrifugation showed that the protein runs slower than the *Mj* enzyme (Figure 1, panels C, D). The data for *Af* LDH-like L-MalDH were fitted reasonably well with a single species. The $g(s^*)$ profiles calculated are shown in Figure 1 (panel D). As in the case of the *Mj* enzyme, lowering the protein concentration did not induce the dissociation of *Af* LDH-like L-MalDH. The calculated $s_{20,w}$ values in 25 mM sodium phosphate displayed a linear relathionship in a protein concentration range from 0.05 up to 5 mg/mL (Figure 2). The *Af* LDH-like L-MalDH $s_{20,w}$ value extrapolated to zero concentration was 4.2 S in 25 mM sodium phosphate. This value is the same as obtained for a dimeric mutant of the *Hm* LDH-like L-MalDH (*20*) and close to the value obtained for the dimeric intermediate of L-LDH upon dissociation of the wild-type tetrameric protein following incubation in 1 M guanidinium chloride (*32*). The fitting by the $g(s^*)$ profils provided a molecular mass of 57 kDa, lower but very similar to the expected value of 63 kDa for a dimer. These data show that the *Af* LDH-like L-MalDH is a dimer at 20 °C.

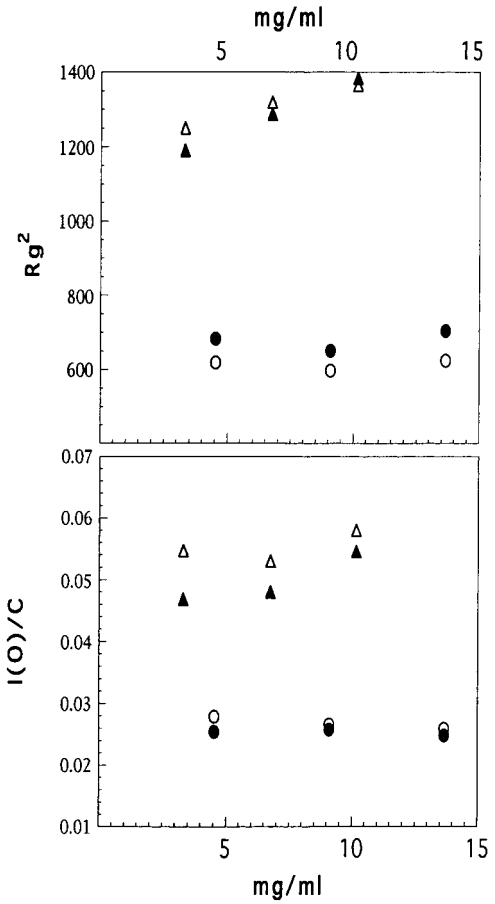

FIGURE 3: Neutron scattering characterization of *A. fulgidus* and *M. jannaschii* LDH-like L-MalDH. The square of the apparent radius of gyration, Rg^2_{app} (upper part), and forward intensity, $I(0)/c_2$ (lower part), obtained from Guinier plots are plotted as function of protein concentration. The data were monitored at 25 °C (open symbols) and 70 °C (closed symbols) for *Af* (circles) and *Mj* (triangles).

The high temperature and salt concentration have been described to drive the oligomerization pathway of the hexameric glutamate dehydrogenase from *Pyrococcus* sp KOD1 (*26*) and the tetrameric formyltransferase from *Methanopyrus kandleri* (*27*). We have therefore checked whether similar mechanisms exist within the dimeric *Af* LDH-like L-MalDH.

High potassium phosphate concentrations enhance strongly the stability the *Af* LDH-like L-MalDH against thermal deactivation (*24*). To probe if this effect was not related to a salt-induced tetramerization, we tested, by AUC, the oligomeric state of the recombinant *Af* LDH-like L-MalDH at three increasing phosphate salt concentrations at 20 °C using a protein concentration of 0.5 mg/mL. The migration profiles were well fitted with a single species in solution for all the salt concentration tested. At 0.1, 0.48, and 0.88 M KH_2PO_4 buffered at pH 9, the experimental values of *s* were 3.8, 2.5, and 1.5 S, respectively. We calculated the $s_{20,W}$ considering a three-component system (protein, salt, and water). The solvation layer associated to the protein is negligible at low salt concentration but not at high concentration (*33*). The calculated values of solvation based upon amino acid composition is generally considered to be accurate. A value of 0.4 g of water/g of protein was calculated using Sedntrep. After correction for density,

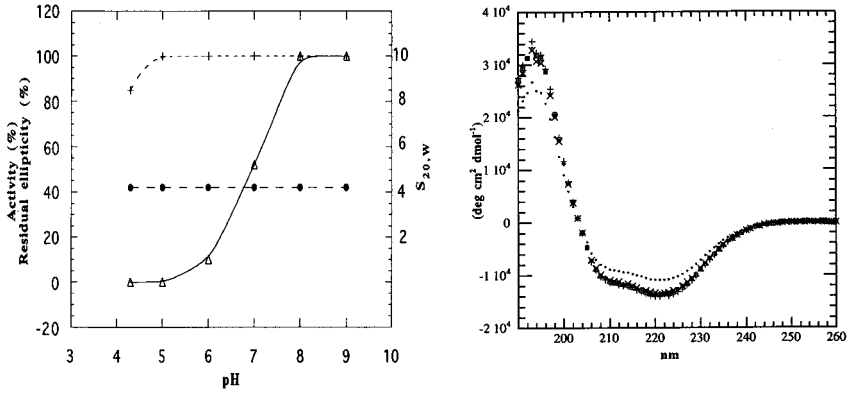

FIGURE 4: pH-dependent active−inactive transition of the dimeric *A. fulgidus* LDH-like L-MalDH. In panel A, the enzymatic activity (triangles), $s_{20,w}$ values (black circles), and the residual molar ellipticity at 222 nm (crosses) were monitored at various pH values. The full enzymatic activity and the molar ellipticity at 222 nm were normalized as % of the values obtained at pH 8. The $s_{20,w}$ values were derived from time derivative analysis determined at a protein concentration of 0.6 mg/mL. The molar ellipticity was taken from spectra presented in panel B. In panel B are shown far-UV circular dichroïsm spectra of *Af* LDH-like L-MalDH at 0.6 mg/mL incubated at pH 9 (×), pH 8 (+), pH 7 (◇), pH 6 (×), pH 5 (⊡), and pH 4.3 (●).

viscosity, and solvation, a constant $s_{20,W}$ value of ≈4.1 S was calculated. Clearly, the protein remained dimeric. The high phosphate concentration effect on the *Af* LDH-like L-MalDH thermal properties is in agreement with the general stabilizing properties of salting-out salts but not related to the oligomerization of dimers.

The SANS experiments were used to probe the putative effect of temperature on the oligomeric state of *Af* LDH-like L-MalDH. When compared to the tertameric *Mj* enzyme, the $I(0)/c_2$ values obtained at 25 and 70 °C for the *Af* LDH-like L-MalDH are approximatively lowered by a factor of 2 in agreement with the AUC results demonstrating that the *Af* [LDH-like] L-MalDH is a dimer. The values of 25 and 26 Å obtained for the radius of gyration at 25 and 70 °C respectively, are very similar and clearly indicated that the oligomeric state was not thermally modified. These Rg_{app} values of ≈25 Å for the dimeric WT *Af* LDH-like L-MalDH are essentially identical to the one measured (24 Å) with the recombinant dimeric *Hm* LDH-like L-MalDH (*20*). There is therefore no temperature-dependent tetramerization of the wild-type dimeric *Af* LDH-like L-MalDH.

We also tested, using SANS, the effect of the coenzyme on the oligomeric state of the *Af* LDH-like L-MalDH. We chose a ratio of 12 NADH/active site, assuming that all the sites would be saturated. The addition of 2.5 mM NADH to a sample of 12 mg/mL incubated at 70 °C did not modify the Rg_{app} or $I(0)/c_2$ of the protein, which, therefore, remains in its dimeric state.

In Af LDH-like L-MalDH a Loop Deletion Modifies the Quaternary Structure. The sequence alignment (Figure 5, panel A) of the three archaeal LDH-like L-MalDH, analyzed in the light of the *Hm* crystallographic structure (*12*), helps one to understand why the *Af* LDH-like L-MalDH cannot reach the tetrameric state.

In the *Af* sequence there is a large gap between strand βH and helix α1G. The equivalent sequence in the *Hm* enzyme corresponds to a loop (residues 205−211) located at the interface between the dimeric units (AB and CD) making a tetramer (Figure 5, panel B). In the *Hm* enzyme, the R207 residue interacts with D211 to make a complex salt bridge cluster involving intra- and intermonomeric interactions. This loop is also acting as a chloride binding site, which uses K205 as ligand. In the *Hm* enzyme there is another R residue at position 292 involved in a second salt bridge cluster that also contributes to the tetramerization. The R292 is involved in an intramonomeric interaction with E301 and in an intermonomeric interaction with D209. In the *Af* enzyme, this kind of interaction was not conserved because there is a K residue at position 292 instead of R, and the D residue is absent due to the reorganization of the connecting loop βH−α1G. Disruption of these clusters by site-directed mutation of both the R207 and R292 has allowed to trap, in certain conditions, the dimer species of the *Hm* LDH-like L-MalDH (*20*). In the *Af* enzyme it is obvious that the absence of such a loop prevents the association of dimeric species to establish a higher level of oligomerization. A sequence alignement of 30 LDH-like L-MalDH (not presented) has shown that this loop deletion is a specific feature of the *Af* enzyme.

There is no charged residue within the tetrameric *Mj* LDH-like L-MalDH at a position equivalent to those involved in the dimer−dimer ionic network of the *Hm* LDH-like L-MalDH. This observation suggested that, at the *Mj* dimer−dimer interface, nonelectrostatic interactions have been selected in the course of evolution. The *Mj* LDH-like L-MalDH and the L-LDH from the hyperthermophilic bacterium *Thermotoga maritima* (*Tm*) have strong sequence similarities (*24*, *25*). The *Tm* L-LDH crystallographic structure shows a slight increase in the number of intra-subunit ion pairs compared with mesophilic L-LDH (*34*). Only one of the seven arginine residues involved in ion pair formation in the *Tm* L-LDH was conserved in *Mj* LDH-like L-MalDH. With *Mj* LDH-like L-MalDH, the arginine distribution throughout the sequence is different, making impossible the prediction of their spatial arrangement. It has been suggested that an additional "thermohelix" located at the dimer−dimer interface making a tetramer may stabilize the *Tm* L-LDH (*34*). The use of secondary structure prediction programs was unsuccessful to describe if an equivalent "thermohelix" exists in *Mj* LDH-like L-MalDH.

pH-Dependent Enzymatic Properties of the Dimeric Af LDH-like L-MalDH. Until now, the tetrameric *Hm* LDH-like L-MalDH is the only enzyme from this group for which a crystallographic structure is known. It can be seen as a dimer of dimers, maintained by a network of ionic interactions (*11*, *12*). This network was disrupted by site-directed

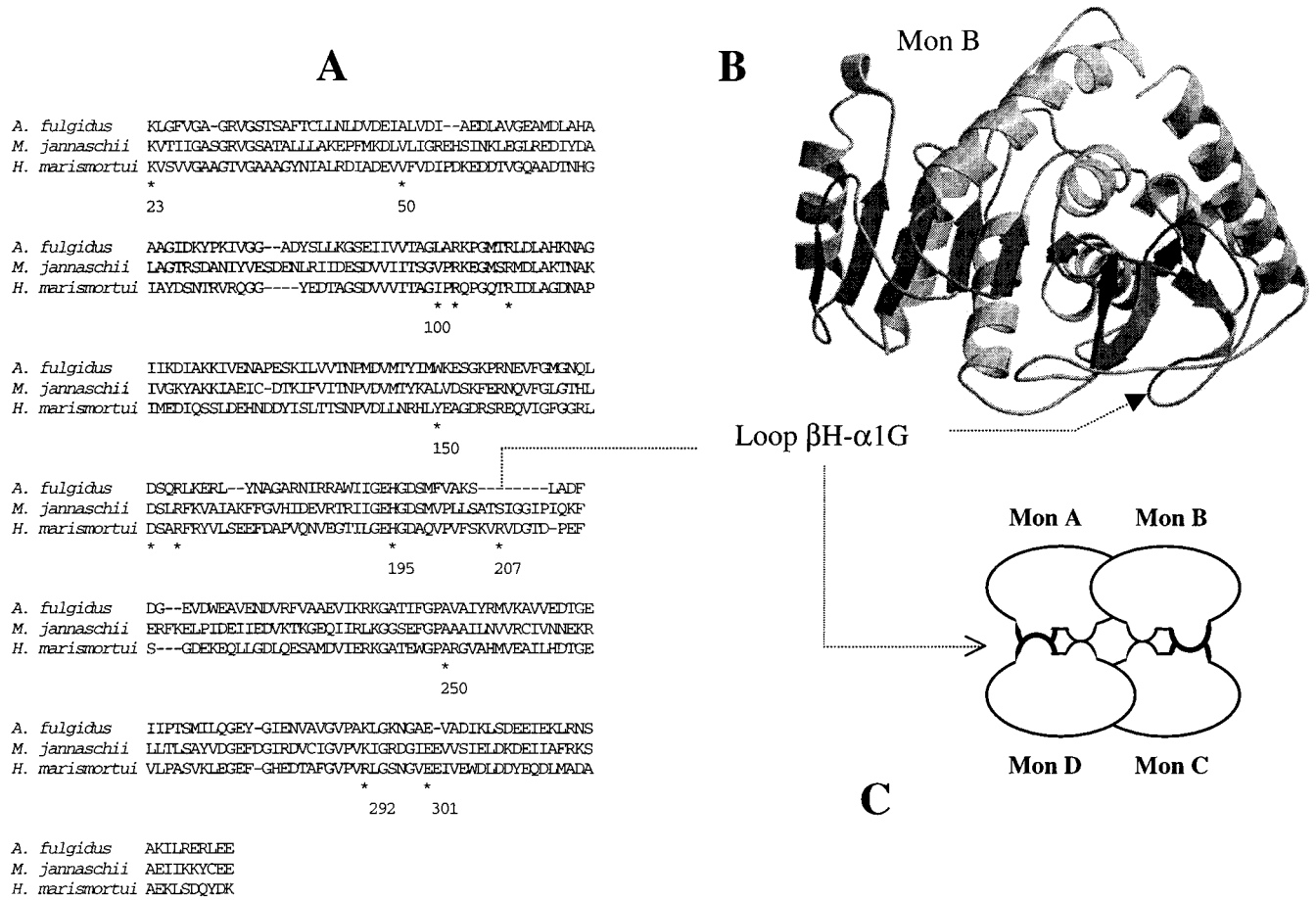

FIGURE 5: Comparative analysis of archaeal LDH-like L-MalDH. In panel A is the sequence alignment of *Af*, *Mj*, and *Hm* LDH-like L-MalDH. The numbering of residues is according to the L-LDH and L-MalDH superfamily (*5*, *12*). Some residue numbers are not used (82, 104, 300), and in cases where the same number refers to more than one amino acid residue these are distinguished by letters (e.g. 29A, 29B, 54A, 54B, 54C, 132A, 132B, 210A, 210B). The stars indicate the strictly conserved active site residues in L-MalDH (R102, R109, D168, R171, and H195) and those which are discussed in the text. In panel B is the crystallographic structure of the *Hm* LDH-like L-MalDH, monomer B (*12*). The loop βH$\angle\alpha$1G is indicated by a black arrow. In panel C, the location of the loop at the interface between the dimers (AB) and (DC) that make a tetramer is in bold on the schematic drawing of the *Hm* enzyme.

mutagenesis leading to trap, in certain conditions, a dimeric species that was characterized as active or inactive depending on pH (*20*). We monitored if this pH effect was observable with the dimeric recombinant *Af* LDH-like L-MalDH, too.

The activity was measured at various temperatures (not all shown) over the pH range of 4.3−9. As it was observed with the recombinant *Hm* dimeric enzyme, a strong loss of activity at 70 °C for the *Af* LDH-like L-MalDH was observed when the standard enzymatic assay was performed below pH 8. To probe the oligomeric state of the *Af* LDH-like L-MalDH, the sedimentation coefficient was determined over the same pH range. The $s_{20,w}$ value = 4.2 S is constant over the pH range 4.3−9, indicating that the *Af* enzyme is always a dimer at these conditions. The far-UV CD spectrum of the *Af* LDH-like L-MalDH showed a broad negative dichroism band centered at 210−220 nm, with an amplitude of $\geq$14 000 deg cm^2 dmol^{-1} (Figure 4). They were identical over the pH range from 9 to 5. The small change observed at pH 4.3 may probably reflect the beginning of the transition toward the unfolded state as it has been observed with proteins at low pH in general. Correlated with the AUC and CD measurements, these enzymatic tests suggested that the dimeric *Af* LDH-like L-MalDH exists as active or inactive structures

The pH-dependent transition of the recombinant *Af* LDH-like L-MalDH between an active and inactive dimeric state without observable conformational changes could be analyzed to a change in the ionization state of the critical active histidine residue with a p*K* value between 6 and 8. In L-LDH and L-MalDH in general, this strictly conserved His at position 195 acts as a proton donor−acceptor (*5*). This transition from the active to the nonactive enzyme has already been observed at pH values between 8 and 7 with the dimeric *Hm* LDH-like L-MalDH obtained by mutagenesis but is not observable with the wild-type tetrameric *Hm* enzyme (*20*).

Our data suggest that the oligomeric dimeric state within the LDH-like group of L-MalDH displays specific properties compared to the dimeric mitochondrial and cytosolic subgroup of L-MalDH. The dimers display also pH-dependent enzymatic properties. The transition between active and inactive dimers, however, was the consequence of a reversible pH-dependent dissociation into monomers (*35*−*37*).

DISCUSSION

According to the stoechiometry characterized for *Chloroflexus aurantiacus*, *Haloarcula marismortui*, and *Bacillus israeli* enzymes, which belong to the LDH-like group of

L-MalDH (*7*, *23*, *38*), the *Mj* enzyme is a tetramer. The L-MalDH from *Rhodobacter capsulatus* (*Rc*) and *Sulfolobus acidocaldarius* (*Sa*) have been purified and characterized as tetramers (*39*, *40*). Their genome sequencing is in progress and accessible from the GOLD web site at http // igweb.integratedgenomics.com. It is possible to characterize both *Rc* and *Sa* L-MalDH as members of the LDH-like group of L-MalDH, in a similarity sequence search (not shown), by using the *Mj* LDH-like L-MalDH sequence as a query. In contrast to this, the *Af* enzyme remains the only example of dimeric LDH-like L-MalDH. Such an exceptional oligomeric state is probably related to the deletion of a loop involved in the assembly of the tetramer. This work suggested that within the L-MalDH family, there is a strong link between primary sequence and oligomeric state. The tetrameric state is favored when L-MalDH sequences dispay strong similarity with L-LDH rather with sequences from the mitochondrial and cytosolic group of L-MalDH.

Primary sequence and oligomeric state analyses have been used to discriminate between subgroups of the L-MalDH family. To this we can now add the analysis of a further property, the pH-dependent activity only observable at the dimeric level. In the case of the LDH-like group, this pH-dependent enzymatic activity occurs without dissociation of the dimer. In contrast, in other L-MalDH members, enzymatic activity is coupled to a pH-dependent dissociation of dimers into monomers.

NOTE ADDED IN PROOF

The crystal structure of the *Methanococcus jannaschii* LDH-like L-MalDH was published recently in ref *41*.

REFERENCES

1. Huynen, MA., Dandekar, T., and Bork, P. (1999) *Trends MicroBiol. 7*, 281−291.
2. Honka, E., Fabry, S., Niermann, T., Palm, P., and Hensel, R. (1990) *Eur. J. Biochem. 188*, 623−632.
3. Thompson, H., Tersteegen, A., Thauer, R. K., and Hedderich, R. (1998) *Arch. Microbiol. 170*, 38−42
4. Graupner, M., Xu, H., and White, R. H. (2000) *J. Bacteriol. 182*, 3688−3692
5. Goward, R. C., and Nicholls, D. J. (1994) *Protein Sci. 3*, 1883−1888.
6. Sundaram, T. K., Wright, I. P., and Wilkinson, A. E. (1980) *Biochemistry 19*, 2017−2022.
7. Bonneté, F., Ebel, C., Zaccai, G., and Eisenberg, H. (1993) *J. Chem. Soc., Faraday Trans. 89*, 2659−2666.
8. Hall, M. D., Levitt, D. G., and Banaszak, L. (1992) *J Mol. Biol. 226*, 867−882.
9. Carr, P. D., Verger, D., Ashton, A. R., and Ollis, D. L. (1999) *Structure 7*, 461−475.
10. Roger, A. J., Morrison, H. G., and Sogin, M. L. (1999) *J. Mol. Evol. 6*, 750−755.
11. Dym, O., Mevarech, M., and Sussman, J. L. (1995) *Science 267*, 1344−1346.
12. Richard, S., Madern, D., Garcin, E., and Zaccai, G. (2000) *Biochemistry 39*, 992−1000.
13. Cendrin, F., Chroboczek, J., Zaccai, G., Eisenberg, H., and Mevarech, M. (1993) *Biochemistry 32*, 4308−4313.
14. Boernke, W. E., Sanville-Millard, C., Wilkins-Stevens, P., Kakar, S. N., Stevens, F. J., and Donnelly, M. I. (1995) *Arch. Biochem. Biophys. 332*, 43−52.
15. Nishiyama, M., Birkoft, J. J., and Beppu, T. (1993) *J. Biol. Chem. 261*, 14178−14183.
16. Chapman, A. D. M., Cortés, A., Dafforn, T. R., Clarke, A. R., and Brady, R. L. (1999) *J. Mol. Biol.* 285, 703−712.
17. Breiter, D. R., Resnik, E., and Banaszak, L. J. (1994) *Protein Sci. 3*, 2023−2032.
18. Schepens, I., Decottignies, P., Ruelland, E., Johansson, K., and Miginiac-Maslow, M. (2000) *FEBS Lett. 471*, 240−244.
19. Shaw, S., Geyer, R., and Alter G. M. (2000) *Biochim. Biophys. Acta 1478*, 248−256.
20. Madern, D., Ebel, C., Mevarech, M., Richard, S. B., Pfister, C., and Zaccai, G. (2000) *Biochemistry 39*, 1001−1010.
21. Synstad, B., Emmerhoff, O., and Sirevag, R. (1996) *Arch. Microbiol. 165*, 346−353.
22. Naterstad, K., Lauvrak, V., and Sirevåg, R. (1996) *J. Bacteriol. 178*, 7047−7052.
23. Wynne, S. A., Nicholls, D. J., Scawen, M. D., and Sundaram, T. K. (1996) *Biochem. J.* 317, 235−245.
24. Langelandsvik, A. S., Steen, I. H., Birkeland, N. K., and Lien, T. (1997) *Arch. Microbiol. 168*, 59−67.
25. Madern, D. (2000) *Mol. Microbiol. 37*, 1515−1520.
26. Abd Rahman, R. N., Fujiwara, S., Takagi, M., Kanaya, S., and Imanaka, T. (1997) *Biochem. Biophys. Res. Commun. 241*, 646−652.
27. Shima, S., Tziatzios, C., Schubert, D., Fukada, H., Takahashi, K., Ermler, U., and Thauer, R. K. (1998) *Eur. J. Biochem. 258*, 85−92.
28. Kim, R., Sandler, S. J., Goldman, S., Yokota, H., Clark, A. J., and Kim, S. H. (1998). *Biotech Lett. 20*, 207−210.
29. Jacrot, B., and Zaccai, G. (1981) *Biopolymers 20*, 2413−2426.
30. Zaccai, G., and Jacrot, B. (1983) *Annu. Rev. Biophys. Bioeng. 12*, 139−157.
31. Philo, J. S. (2000) *Anal. Biochem. 279*, 151−163.
32. Jaenicke, R., Vogel, W., and Rudolph, R. (1981) *Eur. J. Biochem. 114*, 525−531.
33. Eisenberg, H. (1990) *Eur. J. Biochem. 187*, 7−22.
34. Auerbach, G., Ostendorp, R., Prade, L., Kordorfer, I., Dams, T., Huber, R., and Jaenicke, R. (1998) *Structure 6*, 769−781.
35. Bleile, D. M., Schulze, R. A., Harrison, J. H., and Gregory, E. M. (1977) *J. Biol. Chem. 252*, 755−758.
36. Wood, D. C., Jurgensen, S. R., Geesin, J. C., and Harrison, J. H. (1981) *J. Biol. Chem., 256*, 2377−2382.
37. Muller, J., Gorisch, H., and Parkhurst, L. J. (1984) *Biochim. Biophys. Acta 787*, 258−263.
38. Rolstad, A. N., Howland, E., and Sirevåg, R (1988) *J. Bacteriol. 170*, 2947−2953.
39. Ohshima, T., and Sakuraba, H. (1986) *Biochim. Biophys. Acta 869*, 171−177.
40. Hartl, T., Grossebüter, W., Görisch, H., and Stezowski, J. J. (1987) *Biol. Chem. Hoppe-Seyler 368*, 259−267.
41. Lee, B. I., Chang, C., Cho, S.-J., Eom, S. H., Kim, K. K., Yu, Y. G., and Suh, S. W. (2001) *J. Mol. Biol. 307*, 1351−1362.

BI010168C